journal

J. Am. Ceram. Soc., 78 [1] 251–53 (1995)

Role of Fiber Stitching in Eliminating Transverse Fracture in Cross-Ply Ceramic Composites

Tian-Jian Lu and John W. Hutchinson*

Division of Applied Sciences, Harvard University, Cambridge, Massachusetts 02138

A theoretical study of the feasibility of using fiber stitching to prevent transverse matrix cracking in cross-ply ceramic composites is reported. The prototype problem solved is a curved composite beam subject to pure bending (the C-specimen), which develops a transverse tensile stress σ_0 acting across its circumferential midplane. Fiber stitches normal to this plane bridge a circumferential matrix crack lying along the midplane of the specimen. Results are presented for the energy release rate of this matrix crack as a function of a nondimensional parameter characterizing the fiber stitches. Sufficiently large values of this parameter ensure the applicability of the classical ACK (Aveston, Cooper and Kelly) limit for a steady-state matrix crack subject to σ_0. The results obtained can be used to choose the level of stitching such that transverse matrix cracking will be excluded.

I. Introduction

In this note, a plane strain curved beam of cross-ply ceramic laminate subjected to a bending moment M at the ends is considered, as shown schematically in Fig. 1(a) (M is defined per unit width perpendicular to the plane in this figure). The composite beam has inner and outer radii R_i and R_o with thickness $H = R_o - R_i$. A moment with the sense of application shown induces a transverse (radial) tensile stress acting perpendicular to the circumferential planes. Let σ_0 denote the transverse stress acting on the midplane lying halfway between the inner and outer radii, and let $(\sigma_\theta)_{max}$ denote the maximum tensile circumferential stress which occurs at the inner radius. The ratio of σ_0 to $(\sigma_\theta)_{max}$ increases as R_i/R_o decreases, but is always much smaller than unity. For example, assuming material isotropy in the plane of the specimen, $\sigma_0/(\sigma_\theta)_{max} = 0.051$ for $R_i/R_o = 4/5$, 0.087 for $R_i/R_o = 2/3$, and 0.157 for $R_i/R_o = 1/3$. (A formula relating σ_0 and M for the case of circumferential anisotropy is given by Lu *et al.*[2])

Even though the transverse stress σ_0 will be small compared to the stress acting parallel to the specimen, this transverse stress is cause for concern in an unstitched cross-ply, since there is no mechanism to arrest a matrix crack once one becomes critical (see Fig. 2). This has been verified by the analysis of the unbridged circumferential crack lying at the midplane between the inner and outer radii. The normalized energy release rate for an unbridged crack, G_0, increases sharply as the subtending angle, 2θ, increases, as shown in Fig. 3. These results were taken from Ref. 2 and apply to the case of a cross-ply with isotropic elastic properties in the plane of the specimen, where E_c is the cross-ply modulus. The results in Fig. 3 imply that a small unbridged cracklike flaw will grow unstably to a significant length as soon as it becomes critical, as experiments on unstitched C-specimens reveal. Such a cross-ply would be unacceptably susceptible to transverse cracking and the ensuing loss of bending stiffness that would entail. Transverse cross-stitching is required to eliminate transverse matrix cracking, or, at least, to ensure that significant stiffness loss does not accompany transverse matrix cracking.

The problem addressed here is that of the circumferential crack in Fig. 1 bridged by transverse fiber stitches. There are two aspects to the problem. As might be surmised on intuitive grounds motivated by the depiction in Fig. 1(b), the classical ACK[1,3] result for steady-state matrix cracking of a bridged crack applies to this problem if the stitching is adequate. The level of stitching required for applicability of the ACK formula will be obtained. Given this applicability, one can then predict the level of stitching needed to exclude transverse matrix cracking, if that is the objective.

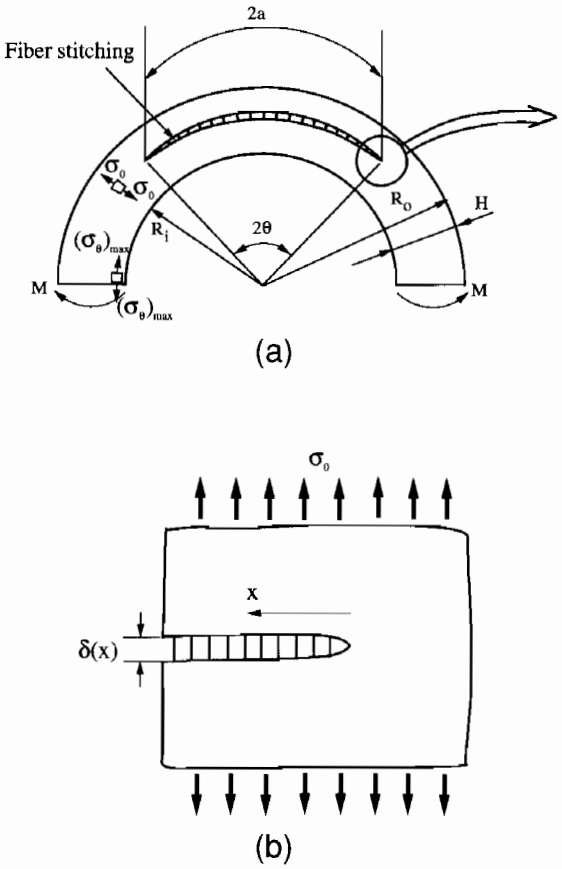

Fig. 1. (a) Conventions for the curved composite beam with fiber stitching across the surfaces of a matrix crack. (b) "Steady-state" matrix crack propagating under stress σ_0.

R. M. McMeeking—contributing editor

Manuscript No. 193475. Received June 20, 1994; approved October 11, 1994.
Supported in part by the ARPA University Initiative ONR Prime Contract No. N00014-92-J-1808 and by the Division of Applied Sciences, Harvard University.
*Member, American Ceramic Society.

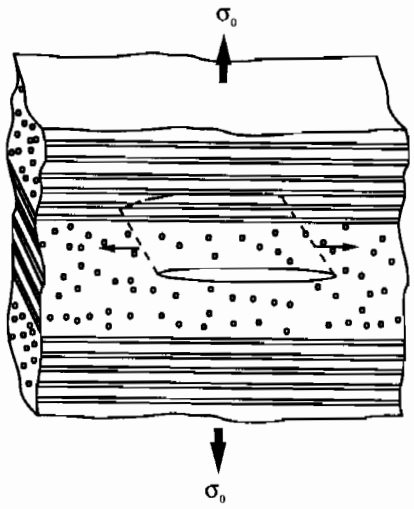

Fig. 2. Schematic illustration of the growth of a transverse matrix crack in a 90° ply.

II. Analysis

The effect of the bridging stitching fibers is modeled in exactly the same way that fiber bridging is treated in the analysis of matrix cracks in unidirectional fiber-reinforced materials. Specifically, the fibers are smeared out and replaced by a continuous distribution of nonlinear springs bridging the matrix crack. The crack length $2a$ and specimen thickness H are assumed to be large compared to the spacing of the stitching fibers. Let (c_f, E_f, R_f) denote the area fraction, axial modulus, and radius of the stitching fibers. The area fraction of stitching fibers will have to be fairly small (i.e., $c_f \leq 0.05$) if stitching is to be feasible. The fibers bridging the circumferential matrix crack are assumed to debond and to slide relative to the surrounding composite, resisted by a constant friction stress τ. Resistance associated with debonding is ignored, as is the effect of any traverse residual stress. The bridging law relating the effective crack opening displacement, $\delta(x)$, at a point x along the crack to the bridging stress, $p(x)$, is[4]

$$p(x) = \beta\sqrt{\delta(x)/2} \tag{1}$$

where

$$\beta = \left\{\frac{4c_f^2 E_f E^2 \tau}{(1 - c_f)^2 R_f E_c^2}\right\}^{1/2} \tag{2}$$

Here, E_c denotes the modulus of the "matrix" surrounding the stitching fibers, which should be identified with the modulus of the cross-ply in the transverse (radial) direction, and $E = c_f E_f + (1 - c_f)E_c$.

The problem of Fig. 1 with Eq. (1) specified along the crack has been analyzed using a finite element formulation, and results will be reported below. If the stitching meets the condition

$$\frac{\beta\sqrt{H}}{\sqrt{E_c\sigma_0}} > 1 \tag{3}$$

it will be seen that the energy release rate G of the crack is well approximated by

$$G_{ACK} = \frac{2\sigma_0^3}{3\beta^2} \tag{4}$$

This is the ACK prediction[1,3] for the situation depicted in Fig. 1(b), where the bridged matrix crack responds to the local midplane stress σ_0 as if it were applied remotely to a straight semiinfinite bridged crack advancing in steady state in an infinite solid. Condition (3) ensures that the substantial crack opening, which would occur for the unbridged crack, will be suppressed by the stitching. This condition also ensures that the major stiffness loss accompanying an unbridged circumferential crack will largely be eliminated.

Continue to let $G_0 \equiv G$ ($\beta = 0$) be the energy release rate of the unbridged circumferential crack plotted in Fig. 3. The energy release rate, G, of the bridged circumferential crack shown in Fig. 1 can be expressed in either of the two following nondimensional forms:

$$G/G_0 = F_1(\theta, \beta\sqrt{H}/\sqrt{E_c\sigma_0}, R_i/R_o) \tag{5}$$

$$G/G_{ACK} = F_2(\theta, \beta\sqrt{H}/\sqrt{E_c\sigma_0}, R_i/R_o) \tag{6}$$

where G_{ACK} is given by Eq. (4). There is also a dependence, not explicitly shown, on the Poisson ratio and on any nondimensional parameters characterizing elastic anisotropy of the cross-ply in the plane of the specimen. The numerical results reported below in Figs. 4 and 5 are restricted to the case of elastic isotropy in the plane with a Poisson ratio of 0.3.

A finite element procedure was used to obtain the crack tip energy release rate as dependent on the stiffness of the stitching fibers. Details of the finite element modeling are similar to those described for the unbridged crack in Ref. 2. The nonlinear bridging law (1) is implemented via the spring element provided in the finite element code ABAQUS. The energy release rate G at the tip of the circular matrix crack is calculated by applying an adaptation of the J-integral. A mesh sensitivity study was conducted to ensure the accuracy of the results reported below.

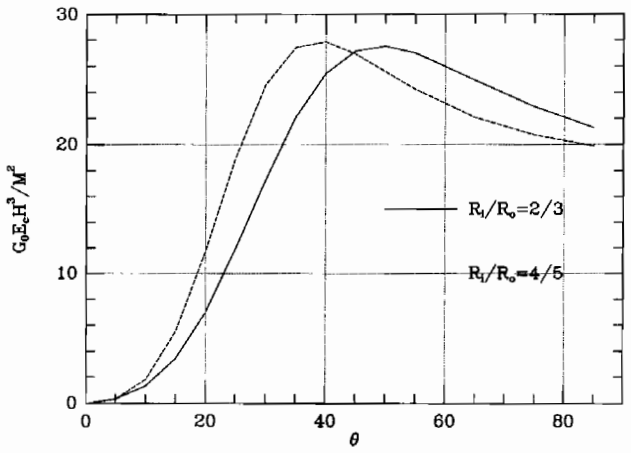

Fig. 3. Normalized energy release rate as a function of θ for an unbridged matrix crack in the curved beam.

III. Results and Discussion

Figure 4 presents the results of the energy release rate as the ratio G/G_0 versus $\beta\sqrt{H}/\sqrt{E_c\sigma_0}$ for $\theta = 30°$ and for two inner-to-outer radius ratios, $R_i/R_o = 2/3$ and $R_i/R_o = 4/5$. The results show that bridging reduces the energy release rate to a small fraction of the value for the unbridged crack for all values of $\beta\sqrt{H}/\sqrt{E_c\sigma_0}$ which are larger than about 0.5. These same results, along with an additional set of results for $\theta = 10°$, are plotted in Fig. 5 as the ratio G/G_{ACK}. This plot reveals the approach of G to G_{ACK} as $\beta\sqrt{H}/\sqrt{E_c\sigma_0}$ increases. As a reasonable approximation, one can estimate G using G_{ACK} when condition (3) is met, and in essentially all cases G_{ACK} provides an upper estimate to G. (The ratio G/G_{ACK} is zero at $\beta\sqrt{H}/\sqrt{E_c\sigma_0} = 0$ because $G = G_0$ at $\beta = 0$, while G_{ACK} is unbounded as β approaches 0.)

To summarize, we consider the simultaneous implications of condition (3), guaranteeing the approximation $G \approx G_{ACK}$, together with the requirement

$$G_{ACK} < (1 - c_f)\Gamma_m \tag{7}$$

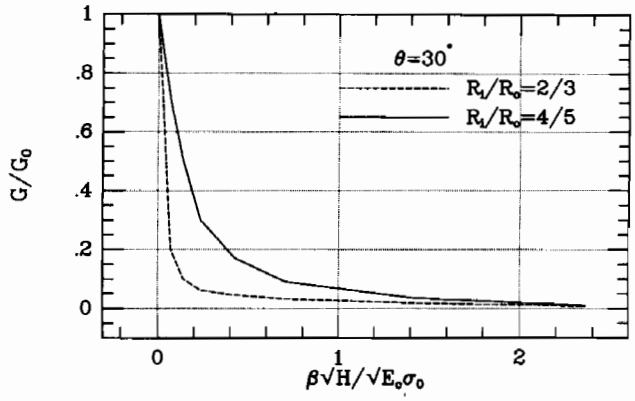

Fig. 4. Ratio of the energy release rate for a bridged crack to that of an unbridged crack plotted against the nondimensional stitching fiber parameter $\beta\sqrt{H}/\sqrt{E_c\sigma_0}$.

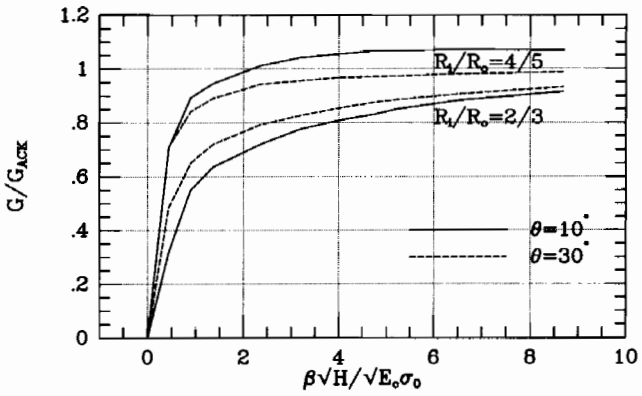

Fig. 5. Normalized energy release rate of the bridged crack versus the nondimensional stitching fiber parameter $\beta\sqrt{H}/\sqrt{E_c\sigma_0}$.

ensuring that transverse matrix cracking does not occur. Here, Γ_m is the effective toughness of the matrix material through which the transverse crack propagates. Condition (3) can be expressed as a requirement on the area fraction of stitching fibers as

$$\frac{c_f}{1-c_f} > \sqrt{\frac{E_c^3}{4E_iE^2}\left(\frac{R_f}{H}\right)\left(\frac{\sigma_0}{\tau}\right)} \qquad (8a)$$

Similarly, condition (7) can be expressed as

$$\frac{c_f}{1-c_f} > \sqrt{\frac{E_c^2\sigma_0^3R_f}{6E_iE^2\tau(1-c_f)\Gamma_m}} = \sqrt{\frac{E_c^3}{4E_fE^2}\left(\frac{R_f}{H}\right)\left(\frac{\sigma_0}{\tau}\right)}\sqrt{\frac{2\sigma_0^2H}{3E_c(1-c_f)\Gamma_m}} \qquad (8b)$$

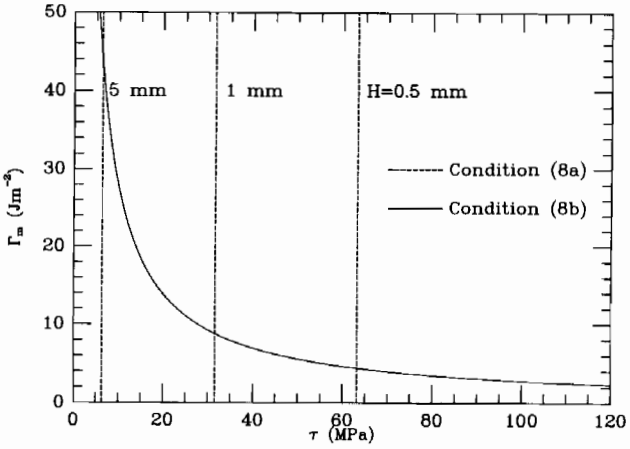

Fig. 6. Combinations of Γ_m and τ that satisfy conditions (8*a*) and (8*b*) given $\sigma_0 = 50$ MPa, $c_f = 0.05$, $E_c = E_i = E = 200$ GPa and $R_i = 7$ μm. To satisfy (8*a*), τ must be to the right of the dashed line for a given H, and to satisfy (8*b*) the combination must lie above the solid-line curve.

As an illustration, consider the following representative values: $E_c = E_f = E = 200$ GPa, $R_f = 7$ μm and $\sigma_0 = 50$ MPa, and assume the area fraction of the fiber stitches is $c_f = 0.05$. Condition (8*a*), ensuring $G \approx G_{ACK}$, is satisfied for all levels of τ to the right of the vertical dashed line in Fig. 6, corresponding to a particular value of specimen thickness H. Condition (8*b*), which excludes the possibility of matrix cracking, is independent of H and is met for all combinations of τ and Γ_m above the solid line curve in Fig. 6. This example emphasizes that careful consideration may have to be given to the level of fiber stitching and the fiber–matrix interface properties if transverse matrix cracking is to be avoided. If one is willing to tolerate matrix cracking as long as there is not a major loss of bending stiffness, then one needs only to satisfy (8*a*). Finally, it has tacitly been assumed that the length of the sliding zone on either side of the matrix crack surface does not reach the inner or outer surfaces of the specimen (i.e., the sliding length is less than $H/2$). This possibility can be checked, but it would be likely only for thin specimens with low levels of τ.

Acknowledgments: The authors would like to thank Y. L. Cui, A. G. Evans, J. R. Rice, and Z. C. Xia for helpful discussions. The commercial finite element code ABAQUS was used in the numerical computation.

References

[1]J. Aveston, G. A. Cooper, and A. Kelly, "Single and Multiple Fracture"; pp. 15–24 in *The Properties of Fiber Composites*, conference proceedings, National Physical Laboratory. IPC Science and Technology Press, Guildford, Surrey, U.K., 1971.

[2]T. J. Lu, Z. C. Xia, and J. W. Hutchinson, "Delamination of Beams under Transverse Shear and Bending," *Mater. Sci. Eng., A*, 1994 (in press).

[3]B. Budiansky, J. W. Hutchinson, and A. G. Evans, "Matrix Fracture in Fiber-Reinforced Ceramics," *J. Mech. Phys. Solids*, **34**, 167–89 (1986).

[4]B. Budiansky, A. G. Evans, and J. W. Hutchinson, "Fiber-Matrix Debonding Effects on Cracking in Aligned-fiber Composites," *Int. J. Solids Struct.*, 1994 (in press). □